

Laminar flame speed simulations of methane-air and n-heptane-air mixtures by using an adapted mechanism

S. Schuh^{*,1}, F. Winter¹

¹Institute of Chemical, Environmental and Bioscience Engineering, Technische Universität Wien, Getreidemarkt 9/166, 1060 Vienna, Austria

Abstract

In the dual fuel combustion process, various types of fuel inhomogeneously distributed within the combustor interact in complex ways with each other. For simulating these processes, a mechanism is necessary that correctly reproduces the interactions of the fuels. Based on the Complete San Diego mechanism with the n-heptane extension [1], a mechanism for the simulation of dual fuel combustion processes is currently under development. The evaluation of the adapted mechanism is performed by comparing calculated and measured ignition delay times of methane-propane-n-heptane mixtures at up to 100 bar. Furthermore, the simulated laminar flame speed of methane-air and n-heptane-air mixtures between 1 and 25 bar is compared with experimental values. It should be noted that the development is not yet completed, the paper reports on the actual status of the adaption process.

Introduction

Worldwide shipping accounts for the emission of around 1 billion tons of carbon dioxide a year, equivalent to 3% of mankind's total carbon dioxide emissions. It is also responsible for 15% of nitrogen oxide emissions and 13% of sulfur dioxide emissions [2]. In port regions, ships contribute significantly to air pollution. To counter this, the regulations on the maximum permitted emission levels are becoming increasingly stringent, especially in coastal regions. In the field of large engines, as used in shipping, the dual fuel combustion process is a promising way to reduce pollutant emissions. In contrast to an ordinary combustion engine with compression ignition, a mixture of air and natural gas is sucked in and compressed in the dual fuel combustion process. At the end of compression of the natural gas-air mixture, a small amount of liquid fuel such as diesel is injected into the combustion chamber to ignite the mixture. In order to optimize the dual fuel combustion process, it is necessary to understand which processes take place in the combustion chamber. However, these are very complex due to the use of different fuels in initially different states of matter and a spatially strong variation of the composition. As part of the "Dual Flame" project funded by the Austrian Research Promotion Agency FFG, the dual fuel combustion process is being examined more closely with the aid of simulations with the aim of being able to reproduce the processes in the combustion chamber. A necessity for the simulative study is the availability of a suitable reaction mechanism.

Reaction mechanism

The mechanism used in this study is based on the Complete San Diego Mechanism with the heptane add-on [1]. To assess the performance of the mechanism, in a first step, a comparison was made between measured and calculated ignition delay times (IDT) of homogeneous methane-propane-n-heptane mixtures by performing 0D-simulations using the software LOGEresearch [3]. –

–The experimental values used were determined with a rapid compression machine (RCM) and a shock tube (ST) at pressure values of 60 and 100 bar. By means of CFD simulations, inhomogeneous mixture compositions were investigated and compared with results from a combustion vessel and rapid compression expansion machine (RCEM) experiments. However, the CFD studies are not part of the discussion in this paper, but more details are available in the publication of Frühhaber et al. [4].

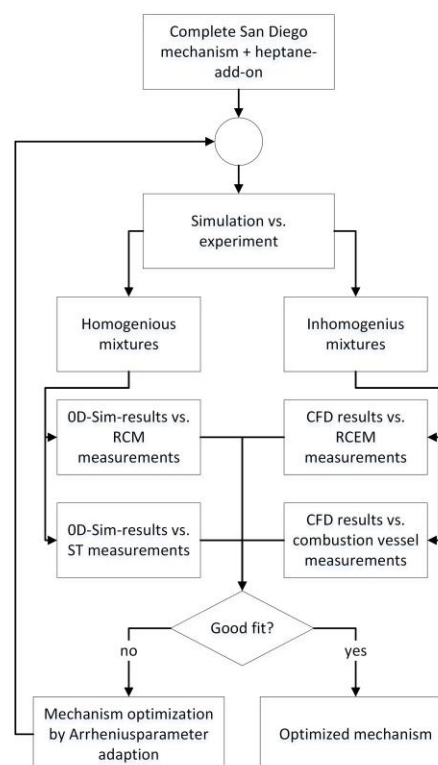


Figure 1: Schematic representation of the adaptation process.

* Corresponding author: sebastian.schuh@tuwien.ac.at
Proceedings of the European Combustion Meeting 2019

An adjustment of the mechanism was initiated when a significant difference between the experimental values and the simulation results was apparent. The adaptation itself was carried out by changing the Arrhenius parameters of specially selected elementary reactions and compound reactions. A schematic representation of the adaptation process can be seen in Figure 1. The selection of the reactions to be adapted was carried out by means of a sensitivity analysis. The influence of the respective reactions on the formation of CH radicals was investigated. These radicals show a distinctive increase in concentration shortly before ignition, which provides a direct indication of which reactions have a major influence on the IDT. The elementary and compound reactions used for the mechanism adaptation considering the calculation of the IDT are summarized in Table 1.

Table 1: Elementary and compound reactions used for the mechanism adaptation considering IDT-data.

No.	Reaction
1	$\text{CH}_4 + \text{OH} \leftrightarrow \text{H}_2\text{O} + \text{CH}_3$
2	$\text{CH}_4 + \text{O}_2 \leftrightarrow \text{CH}_3 + \text{HO}_2$
3	$\text{CH}_4 + \text{HO}_2 \leftrightarrow \text{CH}_3 + \text{H}_2\text{O}_2$
4	$\text{C}_3\text{H}_8 + \text{OH} \leftrightarrow \text{N-C}_3\text{H}_7 + \text{H}_2\text{O}$
5	$\text{C}_7\text{H}_{16} + \text{HO}_2 \leftrightarrow \text{H}_2\text{O}_2 + \text{NC}_7\text{H}_{15}$
6	$\text{NC}_7\text{H}_{15} + \text{O}_2 \leftrightarrow \text{C}_7\text{H}_{14} + \text{HO}_2$
7	$\text{NC}_7\text{H}_{15} + \text{O}_2 \leftrightarrow \text{NC}_7\text{-QOOH}$
8	$\text{NC}_7\text{-QOOH} \leftrightarrow \text{HO}_2 + \text{C}_7\text{H}_{14}$
9	$\text{NC}_7\text{-QOOH} + \text{O}_2 \leftrightarrow \text{NC}_7\text{-OQOOH} + \text{OH}$
10	$\text{NC}_7\text{-OQOOH} \leftrightarrow \text{OH} + \text{CH}_2\text{O} + \text{CO} + \text{C}_2\text{H}_4 + \text{N-C}_3\text{H}_7$

In order to be able to determine which Arrhenius parameters of the individual reactions had to be adapted to achieve an improvement in the result, comparative simulations with an Arrhenius parameter sweep were performed. To ensure that the Arrhenius parameter adjustment was within the allowable range, a comparison of the temperature-dependent reaction rate coefficients with the NIST kinetics database [5] was made, provided that data were available for the particular reaction which is true for the reactions 1 to 4 in Table 1. In the following, Figure 2 to Figure 5 show a comparison of the reaction rate coefficients before (k_{pre}) and after (k_{post}) the mechanism adaptation. Furthermore, the reaction rate coefficient k_{NIST} determined using the NIST database, is given. The calculation of the reaction rate coefficients is performed with the formula (1)

$$k = A \cdot \left(\frac{T}{298 \text{ K}} \right)^\beta \cdot e^{-\frac{E_a}{R \cdot T}} \quad (1)$$

with the frequency factor A in $\text{cm}^{3(n-1)} \text{molecule}^{-1} \text{s}^{-1}$, the order n of the reaction, the gas temperature T in K , the dimensionless temperature exponent β , the activation energy E_a in kJ mole^{-1} and the universal gas constant R in $\text{kJ mole}^{-1} \text{K}^{-1}$. For optical orientation, the illustrations in

the background of Figure 2 to Figure 5 indicate the course of all considered reaction rate coefficients, with this graphical representation being taken from the NIST database. The red shading in the diagram represents the area that lies within the root mean square deviation (RMSD) of the fit function for k_{NIST} determined by an implemented function of the NIST database. The light red shading represents the area with a maximum distance of $2 \times \text{RMSD}$ from the fit function. A total of 85 sources were taken into account when generating the parameter k_{NIST} for the reaction $\text{CH}_4 + \text{OH} \leftrightarrow \text{H}_2\text{O} + \text{CH}_3$. For the selected combination of the Arrhenius parameters for this reaction, it should be noted that the resulting reaction rate constant at temperatures below 300 K lies outside the scattering range of the source data and thus the mechanism should only be used for temperatures $\geq 300 \text{ K}$. To fit the reaction rate coefficient k_{NIST} for the reaction $\text{CH}_4 + \text{O}_2 \leftrightarrow \text{CH}_3 + \text{HO}_2$, 6 sources of the NIST database were used. In the case of reaction $\text{CH}_4 + \text{HO}_2 \leftrightarrow \text{CH}_3 + \text{H}_2\text{O}_2$, the Arrhenius parameters

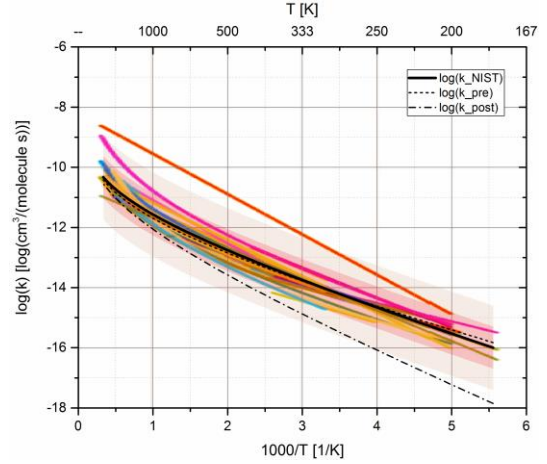


Figure 2: Comparison of the reaction rate coefficient of the reaction $\text{CH}_4 + \text{OH} \leftrightarrow \text{H}_2\text{O} + \text{CH}_3$ before and after adaptation as well as the fit function of the NIST database.

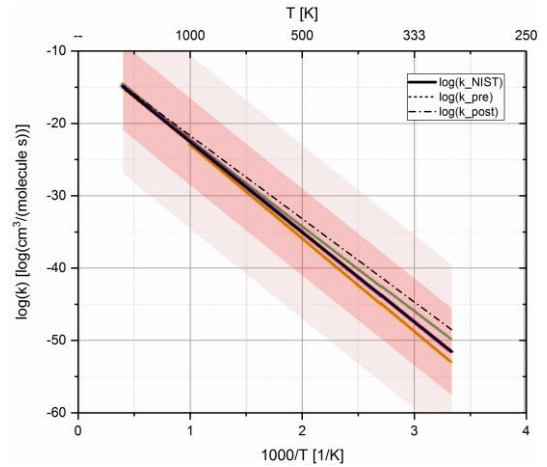


Figure 3: Comparison of the reaction rate coefficient of the reaction $\text{CH}_4 + \text{O}_2 \leftrightarrow \text{CH}_3 + \text{HO}_2$ before and after adaptation as well as the fit function of the NIST database.

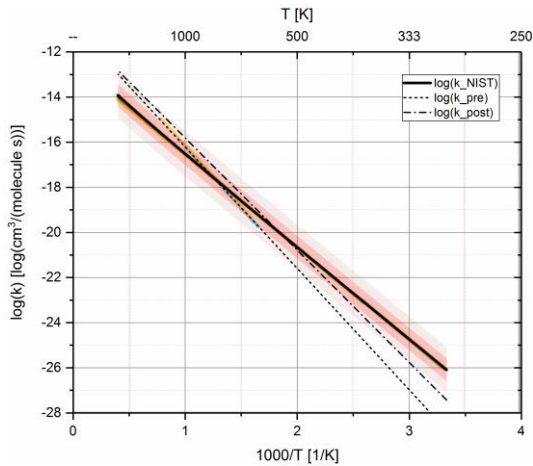


Figure 4: Comparison of the reaction rate coefficient of the reaction $\text{CH}_4 + \text{HO}_2 \leftrightarrow \text{CH}_3 + \text{H}_2\text{O}_2$ before and after adaptation as well as the fit function of the NIST database.

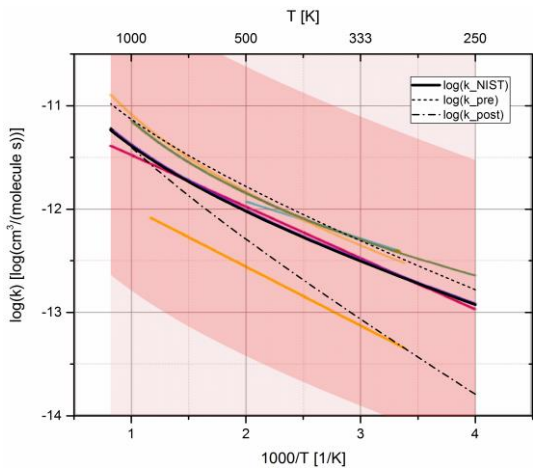


Figure 5: Comparison of the reaction rate coefficient of the reaction $\text{C}_3\text{H}_8 + \text{OH} \leftrightarrow \text{N-C}_3\text{H}_7 + \text{H}_2\text{O}$ before and after adaptation as well as the fit function of the NIST database.

were adjusted so that the resulting reaction rate coefficient lies between the original value k_{pre} and the fitted value k_{NIST} (obtained from the NIST database using 3 sources) for $T < 500\text{K}$ and slightly above k_{pre} for $T > 600\text{K}$. When investigating the influence of propane admixture on the IDT, it was found that the IDT-reducing effect of propane is overestimated by the Complete San Diego mechanism, resulting in too low IDTs. To counteract this, the Arrhenius parameters of the reaction $\text{C}_3\text{H}_8 + \text{OH} \leftrightarrow \text{N-C}_3\text{H}_7 + \text{H}_2\text{O}$ were adjusted. The resulting reaction rate coefficient lies between the fitted k_{NIST} value using 6 sources and the reaction rate coefficient published by Hu et al. [6]. Reactions 5 to 10 in Table 1 are not available in the NIST database to carry out a comparison. Figure 6 shows an overview of the reaction rate coefficients before and after the parameter adjustment. However, a detailed look at these adjustments is not included in this paper.

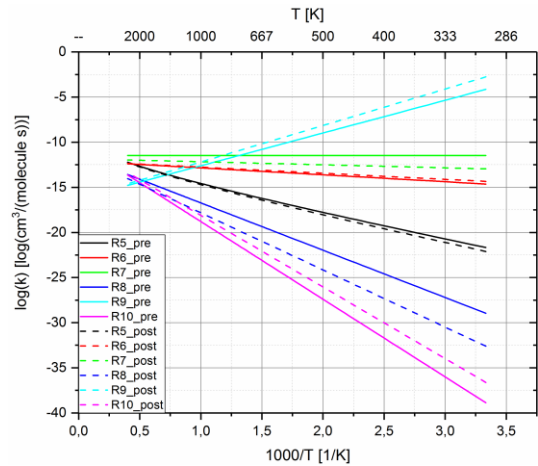


Figure 6: Comparison of the reaction rate coefficients of the reaction 5 to 10 in Table 1 before and after adaptation.

Laminar flame speed simulation

To properly reflect the propagation of the flame front in the combustion chamber in the natural gas-air mixture, the mechanism must be able to calculate the laminar flame speed correctly. In order to evaluate the simulation results, experimentally determined values summarized in a publication of Hashemi et al. [7] were used. In this case, the laminar flame speed of methane-air mixtures at a pressure of 1, 5 and 10 atm, a temperature between 298 and 300 K and a fuel-air equivalent ratio ϕ of 0.55 to 1.7 was examined. The comparison between experimentally determined values and simulated results using LOGEresearch shows an acceptable match for a fuel-air mixture higher than 1.1. At lower ϕ -values, the laminar flame speed is overestimated. In order to determine which elementary reaction has a large influence on the laminar flame speed at low ϕ -values, a ϕ -dependent sensitivity analysis was performed. As a result of this study, the reaction $\text{CO} + \text{OH} \leftrightarrow \text{CO}_2 + \text{H}$ was selected for adaptation. In order to stay within the range of

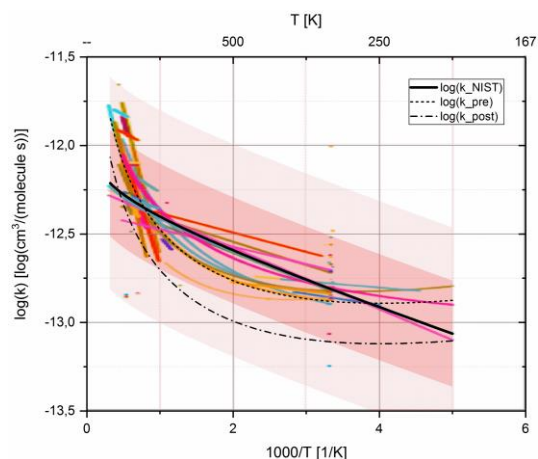


Figure 7: Comparison of the reaction rate coefficient of the reaction $\text{CO} + \text{OH} \leftrightarrow \text{CO}_2 + \text{H}$ before and after adaptation as well as the fit function of the NIST database.

variation of reaction rate coefficients from different sources, a comparison was made with data from the NIST database. The comparison between the reaction rate coefficient before and after the adjustment is shown in Figure 7. It has to be noted, that only data whose permissible temperature range did not start below 200 K were considered for fitting k_{NIST} . A total of 79 sources were taken into account, with data published by Atri et al. [8], Dzegilenko et al. [9] and Herron [10] being used primarily to adjust the Arrhenius parameters. A comparison of the experimentally determined and calculated laminar flame speed using the original Complete San Diego mechanism with the heptane add-on (simulation before adaption) and the adapted mechanism (simulation after adaption) can be seen in Figure 8. The adaptation leads to a reduction of the deviation between simulated and measured laminar flame velocity at ϕ -values < 1.1 . However, the experimental values are not yet accurately reproduced in the entire considered ϕ -range, so there is potential for further optimization for the ongoing adaption process.

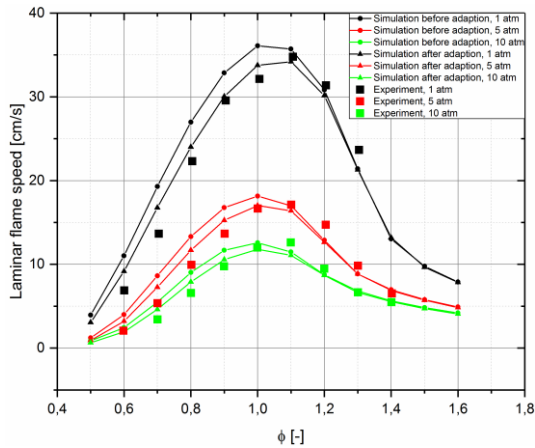


Figure 8: Comparison between measured and simulated laminar flame speed of a methane-air mixture at 299 K and a pressure value of 1, 5 and 10 atm before and after the adaption of the reaction mechanism.

In addition to the propagation of the flame in the methane-air mixture, the flame development directly after the ignition by the injection of a diesel spray is of great importance. Due to this fact, the flame speed in an n-heptane-air mixture was considered, since n-heptane was used as surrogate fuel for diesel in this study. For comparative purposes, experimental values were taken from literature. Jerzembeck et al. [11] have investigated the laminar flame velocity in n-heptane-air mixtures at pressures of 10 to 25 bar, a ϕ -value of 0.7 to 1 and a gas temperature of 373 K. Figure 9 shows a comparison between the experimental data and the simulated results using the unmodified and adapted mechanism. As the comparison shows, at ϕ -values ≤ 0.8 , the adapted mechanism delivers better result than the basic mechanism at all pressures tested. At ϕ -values above 0.8 and a pressure value ≤ 20 bar, the values simulated with the unchanged mechanism are slightly closer to the

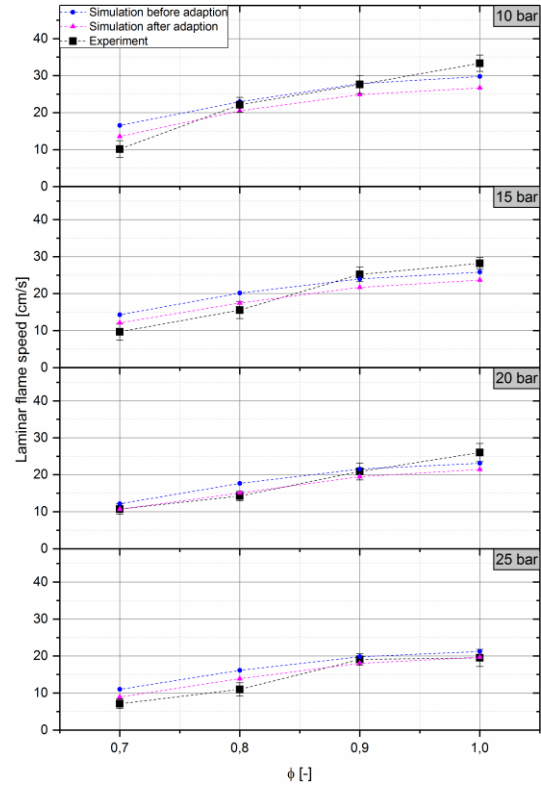


Figure 9: Comparison between measured and simulated laminar flame speed of a n-heptane-air mixture at 373 K and a pressure value of 10, 15, 20 and 25 bar before and after the adaption of the reaction mechanism.

experimental data. At the highest investigated pressure of 25 bar, the adapted mechanism can reflect the experimentally determined values very well and performs better than the basic mechanism for $\phi \leq 0.8$, for $\phi > 0.8$ the original and the adapted mechanism show results within the uncertainty range of the measured values. Nevertheless, the optimization process is not yet completed and a further reduction of the deviation between experiment and simulation results is aspired.

Conclusions

In this study, the current state of development of a mechanisms optimized for dual fuel combustion processes was presented. The adapted mechanism is based on the Complete San Diego mechanism with the heptane add-on. In the first step, the performance of the basic mechanism was evaluated by comparing simulated and measured IDTs. When deviations between experimental and simulated values were found, individual reactions of the mechanism were adapted by changing the Arrhenius parameters. The selection of the respective reactions was made with the help of a sensitivity analysis and comparative simulations. To ensure that the adaptation of Arrhenius parameters was within the allowed limits, a comparison was made with data from the NIST kinetics database. Examination of the laminar flame speed of methane-air mixtures revealed an overestimation at ϕ -values less than 1.1. This overestimation was reduced by adjusting the reaction $\text{CO} + \text{OH} \leftrightarrow \text{CO}_2 + \text{H}$. When simulating n-heptane-air

mixtures, it was found that at ϕ -values ≤ 0.8 , the adapted mechanism provided better results than the basic mechanism. At ϕ -values higher than 0.8, the basic mechanism performed better up to a pressure of 20 bar, at 25 bar the adapted mechanism showed a better reproduction of the experimental values. It should be noted that the mechanism is still under development. When comparing the flame speed, further optimization potential is apparent, as well as in the simulation of the IDTs. With regard to simulation of the flame speed, experimental data at higher pressures will also be considered in the future, such as the flame velocity of methane-oxygen-helium mixtures at 40 and 60 atm published by Rozenchan et al. [12]. Furthermore, some adjustments of individual reactions provide reaction rate coefficients already at the boundary of the scattering range of coefficients from the NIST database, as is the case with reaction $\text{CH}_4 + \text{OH} \leftrightarrow \text{H}_2\text{O} + \text{CH}_3$ and $\text{CO} + \text{OH} \leftrightarrow \text{CO}_2 + \text{H}$, for example. The aim is to keep the adaptation of the individual reactions as small as possible by taking into account further reactions in the ongoing mechanism adaptation process.

Acknowledgements

We would like to show our gratitude to the Austrian Research Promotion Agency (FFG) for funding this work (project number 850690). Further thanks go to LOGE AB for providing the simulation software LOGEresearch.

References

- [1] Chemical-Kinetic Mechanisms for Combustion Applications, San Diego Mechanism web page, Mechanical and Aerospace Engineering (Combustion Research), University of California at San Diego (<http://combustion.ucsd.edu>).
- [2] R. Winkel, U. Weddige, D. Johnsen, V. Hoen, S. Papaefthimiou, Shore Side Electricity in Europe: Potential and environmental benefits, *Energy Policy* 88 (2016) 584-593.
- [3] LOGEresearch, <http://www.logesoft.com>.
- [4] J. Frühhaber, A. Peter, S. Schuh, T. Lauer, M. Wensing, F. Winter, P. Priesching, K. Pachler, Modeling the Pilot Injection and the Ignition Process of a Dual Fuel Injector with Experimental Data from a Combustion Chamber Using Detailed Reaction Kinetics, SAE International, 2018.
- [5] J.A. Manion, R.E. Huie, R.D. Levin, D.R.B. Jr., V.L. Orkin, W. Tsang, W.S. McGivern, J.W. Hudgens, V.D. Knyazev, D.B. Atkinson, E. Chai, A.M. Tereza, C.-Y. Lin, T.C. Allison, W.G. Mallard, F. Westley, J.T. Herron, R.F. Hampson, D.H. Frizzell, NIST Chemical Kinetics Database, NIST Standard Reference Database 17, Version 7.0 (Web Version), Data version 2015.09, National Institute of Standards and Technology, Gaithersburg, Maryland.
- [6] W.-P. Hu, I. Rossi, J.C. Corchado, D.G. Truhlar, Molecular Modeling of Combustion Kinetics. The Abstraction of Primary and Secondary Hydrogens by Hydroxyl Radical, *The Journal of Physical Chemistry A* 101 (1997) 6911-6921.
- [7] H. Hashemi, J.M. Christensen, S. Gersen, H. Levinsky, S.J. Klippenstein, P. Glarborg, High-pressure oxidation of methane, *Combustion and Flame* 172 (2016) 349-364.
- [8] G.M. Atri, R.R. Baldwin, D. Jackson, R.W. Walker, The reaction of OH radicals and HO2 radicals with carbon monoxide, *Combustion and Flame* 30 (1977) 1-12.
- [9] F.N. Dzegilenko, J.M. Bowman, Recovering a full dimensional quantum rate constant from a reduced dimensionality calculation: Application to the $\text{OH} + \text{CO} \rightarrow \text{H} + \text{CO}_2$ reaction, *The Journal of Chemical Physics* 105 (1996) 2280-2286.
- [10] J.T. Herron, Mass - Spectrometric Study of the Rate of the Reaction $\text{CO} + \text{OH}$, *The Journal of Chemical Physics* 45 (1966) 1854-1855.
- [11] S. Jerzembeck, N. Peters, P. Pepiotdesjardins, H. Pitsch, Laminar burning velocities at high pressure for primary reference fuels and gasoline: Experimental and numerical investigation, *Combustion and Flame* 156 (2009) 292-301.
- [12] G. Rozenchan, D.L. Zhu, C.K. Law, S.D. Tse, Outward propagation, burning velocities, and chemical effects of methane flames up to 60 ATM, *Proceedings of the Combustion Institute* 29 (2002) 1461-1470.